

Numerical Analysis of Interaction Between Soils and Pile Group Based on the Full-scale Statnamic Test

Gi-Cheon KANG*, Tetsuo TOBITA and Susumu IAI

*Graduate School of Engineering, Kyoto University

Synopsis

Numerical analysis for interaction between soil and pile group is performed using finite element method with 2D modeling. Results of numerical analysis are compared with the full-scale statnamic test of a 3 x 5 pile group conducted in the Salt Lake City International Airport site. In the numerical analysis of the pile group, there are two cases. The first case is that dynamic loads without cycle static loads. The other is that static loads prior to dynamic loads were applied at the group pile. In results, load versus deflection curves and bending moment versus depth are compared with the measured ones. Also, when numerical analysis includes the static loading before the dynamic loading (Case 2), the load-deflection curves were larger than measured ones but agree better than that of Case 1.

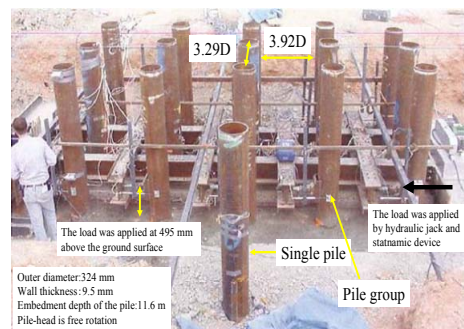
Keywords: Interaction, Numerical analysis, Statnamic test and Pile group

1. Introduction

Considering costs and labors to conduct full-scale lateral load tests on pile groups (e.g., Rollins et al. 1998, 2005), it is desirable to develop a simulation method which can predict group pile response including the group effect with an accuracy required for design practice. Using the 2D FEM code developed by Iai et al. (1992), Tobita et al. (2006) analyzed the full-scale group pile behavior under static lateral loads and obtained reasonable results. Objective of the present study is to further investigate the applicability of the FEM code by simulating the statnamic lateral-load tests conducted in a series of the full-scale lateral-load test project (Rollins et al. 2005).

2. The full-scale lateral load tests of a 3 x 5 pile group

Overall layout of the 15-pile group and single pile is shown in Fig. 1(a). Fig. 1(b) shows the statnamic device for the dynamic load tests.



(a) 15 pile group and a single pile



(b) Statnamic device

Fig. 1 Photograph of the full-scale lateral-load tests

A solid fuel propellant inside the combustion chamber is ignited then the reaction mass and silencer are launched away from the pile group (Snyder 2004).

The soil profile of the site (Fig. 2) shows a dominance of cohesive sandy silt and silty sand. Piles were driven in 3×5 pattern with a spacing of 3.92 pile diameters centre to centre in the direction of loading. The pile is made of steel and has an outer diameter of 324 mm with a wall thickness of 9.5 mm. It was driven closed-ended to a depth of 11.6 m. Lateral load was applied either statically or dynamically. In both cases, a lateral load was applied at 495 mm above the ground surface. Each pile and the load frame were pin-connected so that the rotation was free at the pile head.

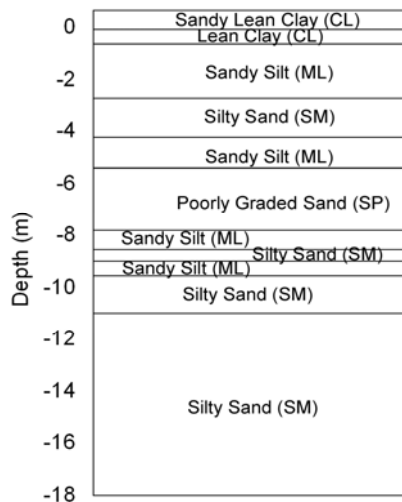


Fig. 2 Ground profile

In the full-scale tests, the static tests on the 15-pile group were conducted simultaneously with the static loading tests. The static tests were performed mainly as final loading cycles. The group pile was cyclically loaded up to certain target deflections after which the static test was performed by loading the pile group to the same target deflection. The dynamic test was performed as a 16th cycle for target deflection of 13 and 25 mm, a 15th cycle for 38 mm, and an 11th cycle for 64 mm target deflection. The static test was performed as an initial cycle once to observe the dynamic behavior of the pile group as it was loaded into virgin soil. Thus, the test was performed as a 1st and 12th cycle for the 89 mm target deflection shown in Fig. 3 (Snyder 2004).

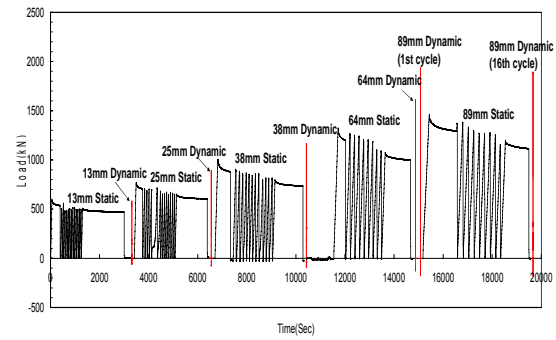


Fig. 3 Loading view of the full-scale test for pile group targeting 13, 25, 38, 64 and 89 mm deflections

3. Numerical model

Two dimensional finite element analysis based on the multi-shear mechanism constitutive relationship, FLIP (Finite element analysis program for Liquefaction Process) (Iai, et al. 1992), is employed to simulate the full-scale lateral-load tests of a pile group. To have the same loading condition with the full-scale tests, the present analysis is conducted under drained condition by applying lateral load at the pile head. In the analysis of the dynamic loading tests, measured time histories of static load are applied to the pile head.

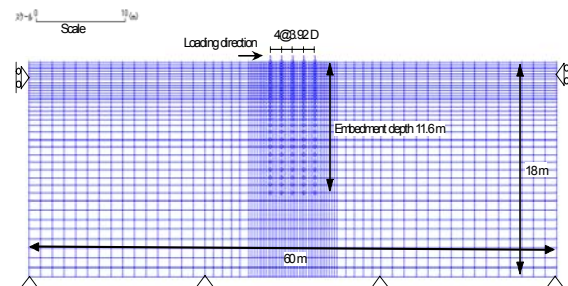


Fig. 4 FEM Mesh for the FLIP analysis

Five piles in the middle row shown in Fig. 1 is a target of the analysis. Finite element mesh of the target cross section is shown in Fig. 4. In FLIP, the multi-spring elements (Towhata and Ishihara 1985) are used for modeling visco-plastic behavior of soils. Bilinear beam elements are used for modeling piles. Displacement degrees of freedom of side boundaries are fixed in horizontal direction, while that of the bottom boundary are fixed in both horizontal and vertical direction. Top and bottom of piles are set as displacement and rotation free to keep the same fixity condition as the full-scale tests.

Soil deformation near piles is a major concern when the simulation is carried out in two dimensions (Iai et al. 2006). In FLIP, soil-pile interaction springs are adapted between soil and pile nodes to take into account the soil deformation

near piles. Values of these spring coefficients are internally determined based on the separately derived empirical relationship. Detail can be found in Ozutsumi et al. (2003).

3.1 Model parameter identification

Soil layers shown in Fig. 2 are adopted in the analysis. Model parameters of the ground and pile are defined based on the geotechnical investigation data at the site (Snyder 2004). Parameters for piles are taken from the industrial standard. Variation of shear modulus in depth is consistent with the variation of tip resistance and sleeve friction of the CPT test results (Tobita et al. 2006). Rayleigh damping parameters are set as 0.15 % for soil by method of trial and error (Fig. 5) and zero for pile element.

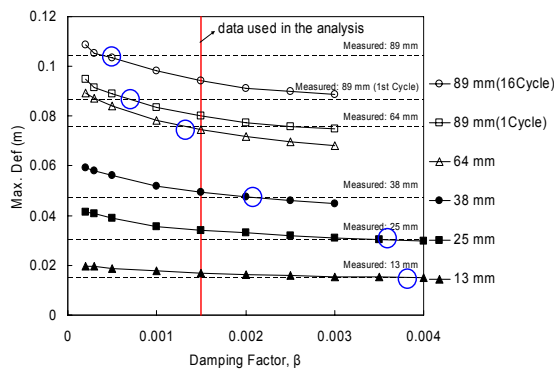


Fig. 5 Determination of Rayleigh Damping factor β

3.2 Single pile behavior

A lateral load is statically applied at the pile head (0.495 m above the surface) until the displacement of 90 mm at the loading point is achieved [Fig. 6(a)]. The maximum load at the maximum deflection agrees, however, the load–deflection behavior is slightly over–estimated. The initial slope of the computed load–deflection curve is about 1.5 times larger than that of measured. Computed load at the pile head deflection of 50 mm is about 30 % over–estimated. The maximum moment at a given lateral load shown in Fig. 6(b) is practically in good agreement.

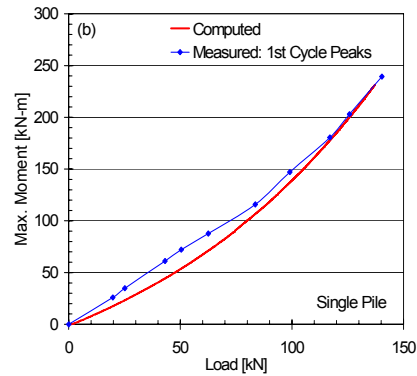
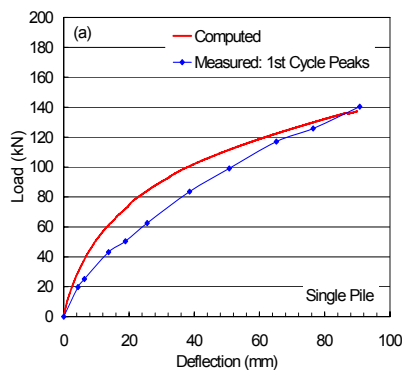


Fig. 6 Single pile: (a) Measured and computed load deflection curve, and (b) Maximum moment load curve

Computed bending moment in depth at 90 mm of the pile head displacement shown in Fig. 7 is consistent with the one measured at the pile head displacement of 89 mm.

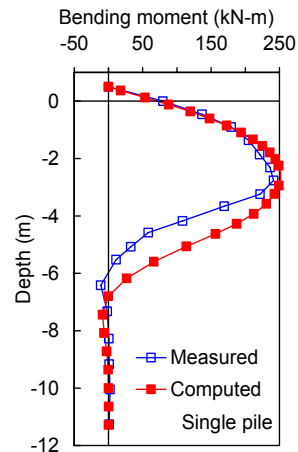


Fig. 7 Comparison of bending moment profile of a single pile: Full scale experiment (Snyder 2004) and computation by FLIP

3.3 Pile group behavior against static loading

In the numerical analysis of the pile group, there are two cases. The first case is that dynamic loads without cycle static loads were sequentially applied to the pile group. The other is that static loads prior to dynamic loads like the field test were applied at the group pile controlled by the separated target deflections.

In Case 1, dynamic loads without cyclic static loads were sequentially applied to the pile group [Fig. 8(a)], i.e., for all target deflections, except for the 1st cycle of target deflection 89 mm. This preserves the simplicity and saves computational time in the numerical analysis. However, deflection levels after the second dynamic loading are evaluated smaller than measured ones [Fig. 8 (b)].

In Case 2, before the dynamic loading, numerical analysis considering static loadings was conducted separately controlled by the target deflections [Fig. 8(c)].

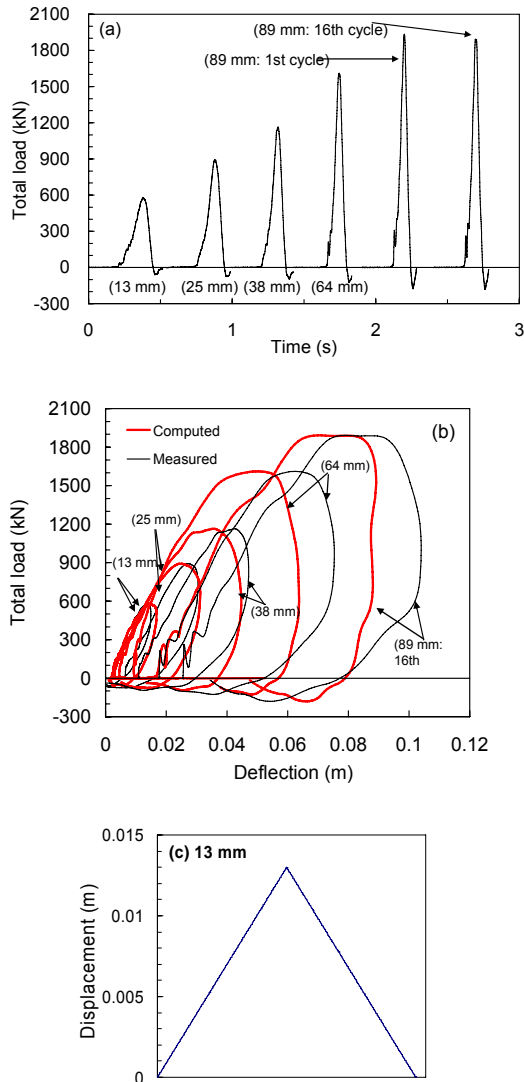


FIG 8. Time sequence of the total load applied to the pile group in the numerical analysis (a), comparison of load–deflection curves except for 1st cycle of a target deflection of 89 mm (b), static load of target deflection 13 mm prior to dynamic loads (c).

3.4 Load versus deflection

Fig. 8 (b) provides the plot of the measured and computed load–deflection curves for all cases, except for the 1st cycle of the target deflection of 89 mm. In each curve, slope in the loading phase agrees well. However, computed curves are consistently under estimating the deflections, partly because loading condition is different from the full–scale tests as mentioned earlier. In the full–scale tests, gaps between piles and surrounding

ground made by static cyclic loads might lead larger deflection, while in the numerical analysis, no gaps are allowed between soil and pile.

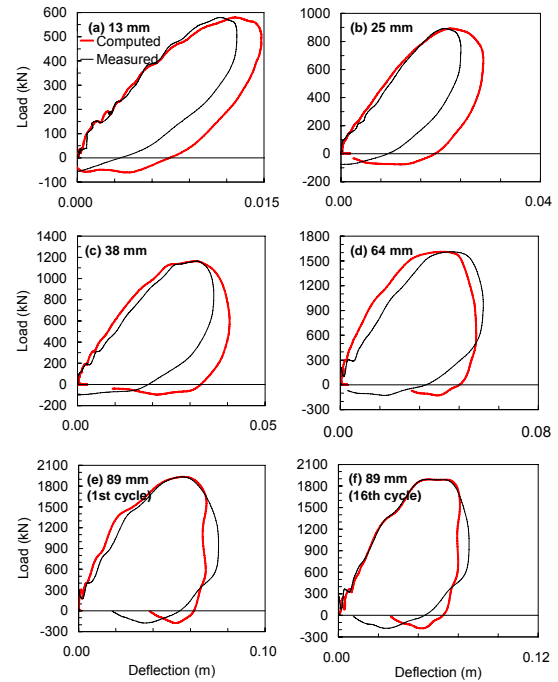


Fig. 9 Measured and computed load versus deflection curve: target deflection of (a) 13 mm, (b) 25 mm, (c) 38 mm, (d) 64 mm, (e) 89 mm (1st cycle), and (f) 89 mm (16th cycle) for Case 1.

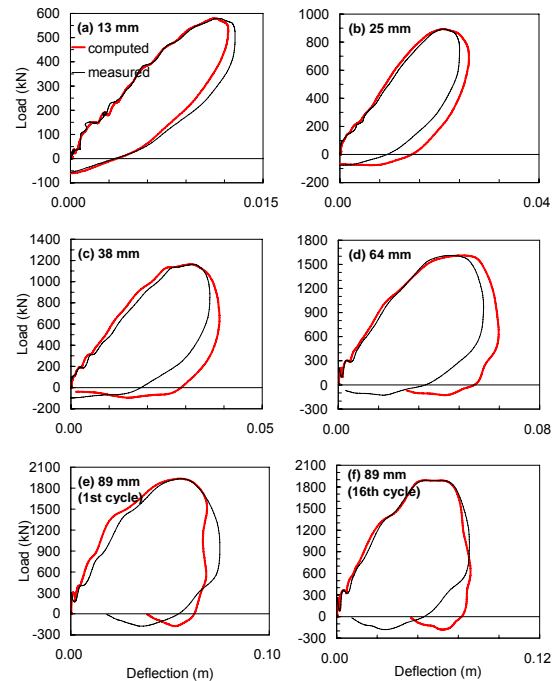
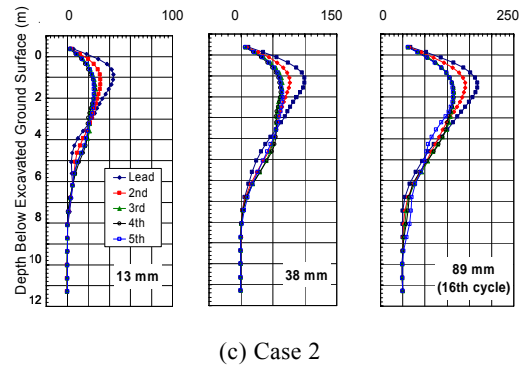
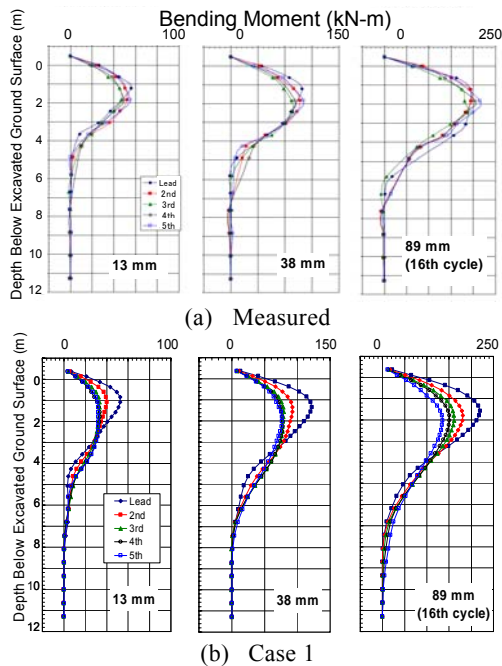


Fig. 10 Measured and computed load versus deflection curve: target deflection of (a) 13 mm, (b) 25 mm, (c) 38 mm, (d) 64 mm, (e) 89 mm (1st cycle), and (f) 89 mm (16th cycle) for Case 2.

Curves shown in Fig. 8(b) are separately shown in Fig. 9 (Case 1). Fig. 10 shows them for Case 2. The 1st cycle of the target deflection of 89 mm is separately shown in Fig. 9 and 10. Each curve is shifted so that loading starts at zero deflection. Load–deflection curves during loading phase agree well for all cases. However, in the unloading phase, deflections are over-estimated for Case 1 than Case 2 when target deflection is small [Fig. 9 (a)-(c)]. As target deflection increases, analytical curves show better agreements, especially, a slope during loading phase agrees well for target deflection 64 mm of Case 2 compared with Case 1.

3.5 Bending moment profiles

Bending moment profiles of target deflections of 13, 38, and 89 mm (16th cycle) are compared in Fig. 11. Snyder (2004) reports that, “in the full-scale static load tests, the depth at the maximum bending moment became progressively greater depths with increasing deflection. This was typically not the case with the dynamic tests.” For example, in Fig. 11, at a target deflection of 13 mm, the peak moments occurred at a depth of 1.8 m for the trailing rows and a depth of 1.2 m for the lead row (Row 1). The peak moments for a target deflection of 89 mm (16th cycle) generally occurred at the same depths. The moment in Row 5 were typically greater than all other rows indicating that the reduced soil resistance ahead of these piles forced them to develop more curvature for a given load resulting in higher bending moments despite the fact that lower loads were carried (Snyder 2004) [Fig. 11 (a)].



(c) Case 2
Fig. 11 Compared with bending moment curves at peak loads for the 13, 38, and 89 mm (16th cycle) target deflection.

In the Case 1 [Fig. 11 (b)], bending moments of trailing row piles show lower peaks than that of the lead row, which is not the case with the full-scale tests shown in measured ones. Compared with measured profile, peak moments of trailing rows are significantly underestimated.

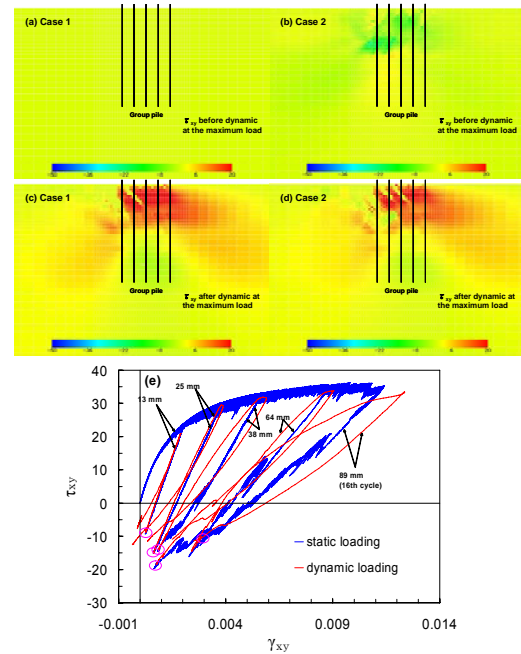


Fig. 12 Shear stress distribution for Case 1 and 2 prior to dynamic loads [(a)-(d)], shear stress-strain curves of Case 2 for all target deflections (e).

In the Case 2 [Fig. 11 (c)], peak moments of all rows are significantly underestimated than Case 1. Also, row 3, 4, and 5 almost give the same ones at large deflections, while bending moment of row 3 gives smallest peak in the full-scale tests.

For explaining the effect of static loads applied to Case 2, the shear stress distributions for target deflection 13 mm were checked in Fig. 12. Fig. 12 (a) and (c) are for Case 1, (b) and (d) are for Case 2. Fig. 12 (b) shows that the shear stress remains before dynamic loading for Case 2 like the real test.

Also, In Fig. 12 (e), the dynamic load starts at a point finishing the static load for Case 2. After all, Case 2 considering static loads like the full-scale tests shows a good agreement than that of Case 1.

4. Conclusions

Needs of development of a simulation method which can predict group pile response including the group effect with the accuracy required to design practice has been increasing. The computer code called FLIP was applied to simulate the full-scale lateral-load tests of a 3 x 5 pile group conducted in the Salt Lake City International Airport site. The soil profile at the test site generally consisted of cohesive sandy silt and silty sand. A series of tests includes static load tests for single and pile group, and dynamic load tests for pile group. Lateral loads were applied at 0.495 m from the ground surface with the hydraulic jack for the static loading and the statnamic device for the dynamic loading. Closed-end steel pipe piles were driven to a depth of 11.6 m. Pile head was rotation free.

In the numerical analysis, model parameters for soils are taken from the geotechnical investigation data at the test site. With these model parameters, the full-scale static loading tests of a single pile and the full-scale dynamic loading tests of a pile group was simulated. Overall load-deflection behavior of the pile group agrees well with the measured ones. When a numerical analysis considering static loadings was conducted separately controlled by the target deflections before the dynamic loading (Case 2), the load-deflection curves were larger and agree better than Case 1. Some discrepancies are found on the bending moment profile. Numerical analysis overestimates the group effects in dynamic tests. This calls up further improvement of a numerical modeling.

References

- Brown, D. A., Morrison, C., and Reese, L. C. (1988): Lateral load behavior of pile group in sand, *Journal of Geotechnical Engineering, ASCE*, 1261–1276.
- Iai, S., Matsunaga, Y., and Kameoka, T. (1992): Strain space plasticity model for cyclic mobility, *Soils and Foundations, Japanese Society of Soil Mechanics and Foundation Engineering*, Vol. 32(2), 1–15.
- Iai, S., Tobita, T., Nakamichi, M., and Kaneko, H. (2006): Soil-pile interaction in horizontal plane, *Seismic Performance and Simulation of Pile Foundations in Liquefied and Laterally Spreading Ground, Geotechnical Special Publication, ASCE*, No. 145, 38–49.
- Ozutsumi, O., Tamari, Y., Oka, Y., Ichii, K., Iai, S., and Umeki, Y. (2003): Modeling of soil-pile interaction subjected to soil liquefaction in plane strain analysis, *Proceedings of the 38th Japan national conference on geotechnical engineering, Akita, Japan, 1899–1990*.
- Reese, L. C., Wang, S. T., Isenhower, W. M., and Arrelage, J. A. (2000): Computer program LPILE plus version 4.0 technical manual, Ensoft, Inc, Austin, Texas.
- Reese, L. C., and Wang, S. T. (1996): Technical manual of computer program GROUP 4.0 for Windows, Ensoft, Inc., Austin, Texas.
- Rollins, K. M., Lane, D. J., and Gerber, T. M. (2005): Measured and computed lateral response of a pile group in sand, *Journal of Geotechnical and Environmental Engineering*, Vol. 131(1), 103–114.
- Rollins, K. M., Peterson, K. T., and Weaver, T. J. (1998): Lateral load behavior of full-scale pile group in clay, *Journal of Geotechnical and Geoenvironmental Engineering, ASCE*, Vol. 124(6), 468–478.
- Snyder, J. L. (2004): Full-scale lateral-load tests of a 3x5 pile group in soft clays and silts, Master thesis submitted to the faculty of Brigham Young University.
- Tobita, T., Iai, S., and Rollins, K. M. (2004): Group pile behavior under lateral loading in centrifuge model tests, *International Journal of Physical Modelling in Geotechnics*, Vol. 4(4), 1–11.
- Tobita, T., Iai, S., and Rollins, K. M. (2006): Numerical analysis of full-scale lateral-load tests of a 3 X 5 pile group, *First European Conference on Earthquake Engineering and Seismology, Geneva, Switzerland*, 700.
- Towhata, I., and Ishihara, K. (1985): Shear work and pore water pressure in undrained shear, *Soils and Foundations*, Vol. 25(3), 73–84.

静・動的な側方荷重を受ける群杭挙動の数値解析

姜 基天*・飛田 哲男・井合 進

*京都大学大学院 工学研究科

要 旨

本研究では、ソルトレーク国際空港で実施された実大群杭の静・動的載荷試験 (Rollins et al. 1998, 2005)を対象として、地盤と群杭の相互作用を明らかにするため、2次元有限要素法を用い数値解析を行った。数値解析では動的な荷重だけを考慮した場合と動的載荷前の静的な荷重も考慮した場合の2種類の解析を行なった。数値解析より得られた荷重-変位関係と曲げモーメント曲線は実験結果と概ね一致した。また、準静的載荷が地盤の応力状態に及ぼす影響を明らかにするため、地盤のせん断応力-ひずみ関係を調べた。その結果、準静的な載荷過程を考慮することで解析の精度が向上することが確認された。

キーワード: 相互作用, 数値解析, 静・動的載荷試験, 群杭